AUIQ Technical Engineering Science

Volume 2 | Issue 2 Article 10

2025

Architectural Optimization of Façade Design Using Nano-Ceramic Films for Green Buildings in Baghdad's Hot Climate

Lina M. Shaker
Laser and Optoelectronics Engineering Department, College of Engineering, Al-Ayen Iraqi University, Nile St, Nasiriyah, Dhi Qar, 64001, Iraq, linamohmmed91@gmail.com

Wan Nor Roslam Wan Isahak
Department of Chemical and Process Engineering, Faculty of Engineering and Built Environment, Universiti Kebangsaan Malaysia, Bangi, Selangor, 43000, Malaysia

Ahmed Salih Mahdi
Research Energy Department, Training and Research Office, Baghdad 10001, Iraq

Recommended Citation

Shaker, Lina M.; Isahak, Wan Nor Roslam Wan; and Mahdi, Ahmed Salih (2025) "Architectural Optimization of Façade Design Using Nano-Ceramic Films for Green Buildings in Baghdad's Hot Climate," *AUIQ Technical Engineering Science*: Vol. 2: Iss. 2, Article 10.
DOI: https://doi.org/10.70645/3078-3437.1039

AUIQ TECHNICAL ENGINEERING SCIENCE 2025;2:155–166

ORIGINAL STUDY

Architectural Optimization of Façade Design Using Nano-Ceramic Films for Green Buildings in Baghdad's Hot Climate

Lina M. Shaker [a,*], **Wan Nor Roslam Wan Isahak** [b], **Ahmed Salih Mahdi** [c]

[a] Laser and Optoelectronics Engineering Department, College of Engineering, Al-Ayen Iraqi University, Nile St, Nasiriyah, Dhi Qar, 64001, Iraq
[b] Department of Chemical and Process Engineering, Faculty of Engineering and Built Environment, Universiti Kebangsaan Malaysia, Bangi, Selangor, 43000, Malaysia
[c] Research Energy Department, Training and Research Office, Baghdad 10001, Iraq

ABSTRACT

This study aims to optimize the architectural integration and energy performance of nano-ceramic window films in a three-story Baghdad commercial building having an overall area of 2,000 m^2. In a 40% window-to-wall ratio (WWR) and climate-responsive orientation, films were selected for solar exposure; north façade overhanging high-transmittance movies, east and west vertical fins on medium-transmittance movies, and south horizontal louvers on low-transmittance movies. Architectural strategies for daylighting, comfort, and façade appearance with low solar heat gain (SHG) were considered. MATLAB 2022 simulations evaluated energy savings, daylight transmission, and solar rejection. The most effective film (either film, HD-IR05100) achieved 29,750 kWh of annual energy savings. The project combines environmental design and the latest façade articulation, proving it possible to achieve passive solar control without compromising visual transparency. 2D technical illustrations and 3D photorealistic renderings support the aesthetic and functional benefits, endorsing nano-ceramic films as a design-led, sustainable solution in tropical climates.

Keywords: Architectural glazing, Nano-ceramic window films, Energy efficiency, Sustainable building, Façade design

1. Introduction

Buildings are the largest power users in the world, and they account for the largest percentage of global energy needs [1]. With the trend, though on the increase in the aftermath of decarbonization policies, becoming stronger, most climate action plans for Arab countries [2], Asian countries [3], the European Union and the United States focus on electrification of heating systems by replacing combustion systems with electric heat pumps [4]. These policies are most relevant for new developments, where efficient systems can be fitted from scratch and where increasing legislative pressure bars the use of natural gas supply pipes [5].

In this evolving energy environment, architectural design is no longer merely a question of performance and aesthetics but also of energy performance and environmental impact [6]. Architectural glass and glazing systems are particularly significant since they help shape the building's energy profile and occupant comfort by selectively controlling the transmittance of solar radiation [7]. Sophisticated recent advancements, such as those explored by Abundiz-Cisneros et al. (2020), demonstrated that aluminum-based optical filters can exhibit good visible light transmittance (VLT) (>80%) with low near-infrared (NIR) transmittance (<20% at wavelengths >1500 nm) with a good cost-benefit ratio [8]. All these advancements emphasize the importance of spectrally

Received 1 June 2025; revised 1 August 2025; accepted 1 August 2025.
Available online 13 August 2025

* Corresponding author.
E-mail address: linamohmmed91@gmail.com (L. M. Shaker).

https://doi.org/10.70645/3078-3437.1039

selective glazing for enhancing both thermal performance and daylighting efficiency through high-precision layer tolerances designed perfectly. In a fascinating twist, solar-abundant grids offer cleaner power during the day [9], when, paradoxically, there is more solar heat gain (SHG) in buildings [10]. Although Lyu et al. (2024) discussed this issue, broader incorporation into architectural paradigms of design is currently limited [11].

In this regard, the application of nano-ceramic window films is an appealing architectural and engineering solution [12]. Architecturally, the integration of nano-ceramic films is advantageous to passive design principles, reducing the reliance on mechanical systems and optimizing visual comfort [13]. These films, composed of ceramic particles that emit far-IR (FIR) radiation (6–14 μm), exhibit superior thermal insulation, mechanical strength, and even biomedical benefits [14]. The ability of ceramic powders to interact with water molecules and stimulate biological activity makes them not only energy-efficient, but also health-conscious design element [15].

The physical principles of window film performance are rooted in the regulation of the four major radiation bands: ultraviolet (UV: 100–400 nm), visible light (VIS: 400–700 nm), solar infrared (IR: 700–3000 nm) [16]. UV-rejection (UVR) technologies prevent material degradation and ensure user health [17]. On the other hand, VLT control is required to maintain daylight quality without contributing to unwanted heat gain [18]. Solar IR control is particularly crucial in climates like Baghdad's [19], w here direct sun exposure causes astronomical cooling loads [20]. Thermal control films, low-emissivity coatings, and smart shading systems collectively address these concerns [21].

In this study, we introduce a context-dependent architectural and energy simulation workflow to assess the yearly energy savings, daylighting functionality, and façade-level optimization of nano-ceramic window films. Through the integration of architectural orientation, climatic conditions, and time-sensitive energy performance, we aim to formulate a performance-driven strategy for glazing selection that balances environmental performance with architectural quality.

2. Methodology

This study proposes a unified approach that combines energy simulation, architectural design measures, and multi-criteria decision analysis (MCDA) for evaluating and optimizing the performance of nano-ceramic window films in building applications. To assess the impact of nano-ceramic window films on building energy performance, a dynamic annual simulation was conducted using MATLAB 2022, employing a custom-developed simulation model based on the heat balance method. This model was implemented through MATLAB's built-in scripting environment and numerical computation capabilities, enabling the simulation of hourly thermal loads and solar heat gains. The simulation setup was designed to simulate a generic medium-sized commercial building in Baghdad, Iraq (Latitude: 33.3°N, Longitude: 44.4°E), that is representative of hot-dry climate conditions as designated by ASHRAE Climate Zone 1B.

The optical properties of the nano-ceramic films VLT, IRR, and UVR were obtained from manufacturer datasheets, Brand name "Sun Vision", Guangdong, China. These values are based on measurements conducted in accordance with ISO 9050:2003, which defines solar and luminous transmittance using spectral weighting under standard solar radiation at normal incidence [22]. This ensures that the reported values are suitable for thermal and daylighting simulations and can be compared consistently across commercial products.

2.1. Climate and solar analysis

Baghdad's hot-arid weather necessitates counteractions to decrease solar heat gain. The average daily global horizontal irradiance (GHI) is approximately 5.5 kWh/m^2/day. Under a clear and sunny day, 85–90% of the sun radiation is mainly direct irradiance, I_D [23]. When it incident upon the PV surface, it decreases as the angle of incidence, θ_i increases by means of the relationship between the direct normal irradiance, I_{DN} of the surface as shown in the equation below:

$$I_D = I_D \cos\theta_i \tag{1}$$

Solar altitude (α) and azimuth (γ) angles were calculated using [24]:

$$a = \sin^{-1}(\cos\varphi \times \cos\delta \times \cos\omega + \sin\varphi \times \sin\delta) \tag{2}$$

$$\gamma = \frac{\sin\alpha \times \sin\varphi - \sin\delta}{\cos\alpha \times \sin\varphi} \tag{3}$$

Using local latitude, φ, solar declination angle, δ and local hour angle, ω. All the above calculations are utilized in calculating the design of shading devices as well as window film selection.

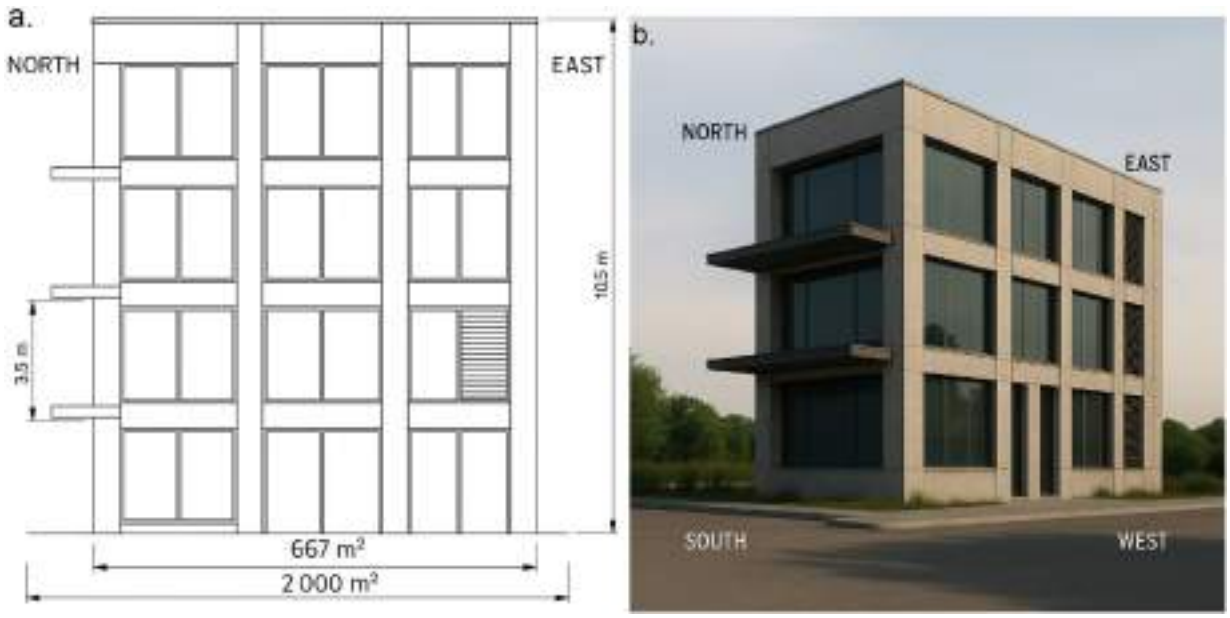

Fig. 1. a. 2D and b. 3D façade rendering showing the orientation and façade-specific application of nano-ceramic films and architectural shading devices.

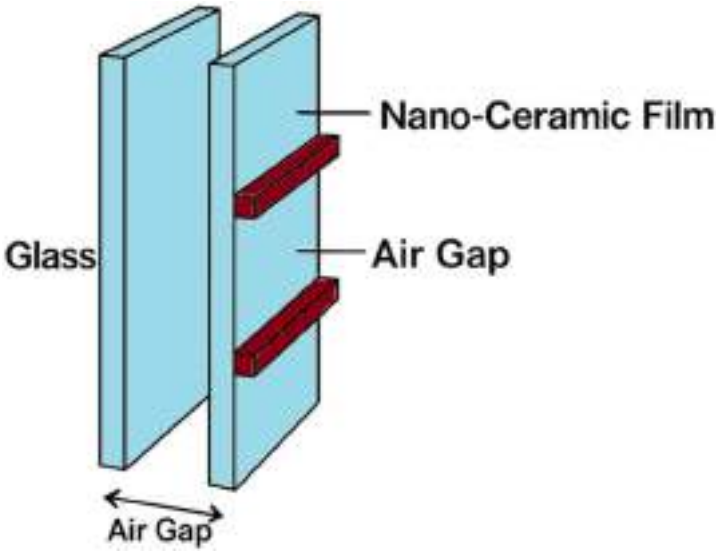

Fig. 2. Schematic cross-section showing the nano-ceramic film layer applied to the double-glazed window system.

2.2. Building geometry and architectural strategy

The modeled building stands at a height of three stories with floor area approximately 667 m^2 per floor with a gross floor area of 2,000 m^2. Floor-to-floor height is 3.5 meters as shown by Fig. 1.a. The window-to-wall ratio (WWR) is uniform at 40% in all the façades. The building is oriented in such a way that the north façade is predominantly oriented to the north, with unrestricted sun exposure on the south, east, and west façades. Shading and film strategies were designed for each orientation north façade, east & west façades, and south façade with fixed horizontal louvers as shown Fig. 1.b. Then a typical double-glazed unit was simulated consisting of two 6 mm glass sheets with a 12 mm air space between them. Nano-ceramic films were applied to the inner surface of the exterior pane as shown in Fig. 2. The optical characteristics of the films, including VLT, IRR, and UVR, were acquired from the manufacturer data.

All nano-ceramic film types were simulated uniformly across orientations, and while the study analyzed energy performance per façade direction, the films themselves were not varied by orientation. The interaction between the horizontal shading devices and the applied films was not parametrically

Table 1. The energy simulation parameters of the work.

Category	Parameter	Value
Climate Zone	ASHRAE 1B	Baghdad, Iraq
Floors	3	Total floor area: 2,000 m^2
WWR	40%	Uniform across façades
Glazing System	Double-pane, clear glass	SHGC = 0.60 (baseline)
HVAC Type	VAV + Reheat	COP = 3.0, Setpoints: 24°C cooling/20°C heating
Internal Loads	0.1 pers/m^2, 10 W/m^2 lighting, 15 W/m^2 equipment	Infiltration = 0.5 ACH
Simulation Controls	10-min timestep, 6 warmup days	Annual run (Jan–Dec)
Shading Devices	Fins (East/West), Overhangs (South)	Reflectivity = 0.5

modeled, and this is acknowledged as a limitation of the current study.

2.3. Energy simulation

The energy performance simulation parameters are presented in Table 1. The simulations accounted for building geometry and orientation, local climate data, internal heat gains, HVAC system design, and glazing properties with and without window films.

The base yearly cooling energy use (E_{base}) without window films was calculated as a reference. The energy savings (E_{saved}) by all types of films were calculated [25]:

$$Energy_{saved} = Energy_{base} \times \left(\frac{\mathrm{SHGC}_{base} - \mathrm{SHGC}_{film}}{\mathrm{SHGC}_{base}} \right) \tag{4}$$

where SHGC is the SHG Coefficient.

The avoided CO_2 emissions were calculated using the following equation, considering Baghdad's LRMCE = 0.5 kg CO_2/kWh, an environmental measure.

$$CO_{2saved} = Energy_{base} \times \mathrm{LRMCE} \tag{5}$$

2.4. Multi-criteria decision analysis (MCDA)

For ranking and selection of the window film options, the Weighted Sum Model (WSM) was employed with multiple criteria E_{saved}, cost savings (C_{saved}), VLT, and glare reduction (GR). Each criterion was normalized:

$$N_{x_{ij}} = \frac{x_{ij} - \min\left(x_j\right)}{\max\left(x_j\right) - \min\left(x_j\right)} \tag{6}$$

The total score (Si) for each film was calculated by the equation:

$$S_i = \sum_{j=1}^{n} \omega_j N_{x_{ij}} \tag{7}$$

Where ω_j is the weight for criterion j, and N_{xij} is the normalized value of criterion j for film i. Weights were assigned based on stakeholder priorities. Weights were assigned using input from three domain experts: an architect, an energy modeler, and a facilities manager at the Renewable Energy and Environment Department – Research Office, Training and Research Office – Ministry of Electricity, Iraq.

A one-way sensitivity analysis was performed by varying each criterion weight by ±10% while holding the others constant, to test the stability of the ranking outcomes. Results indicated that the top-performing alternative (HD-IR05100) remained unchanged under all tested weight variations, confirming the robustness of the decision.

2.5. Correlation analysis

To elucidate the correlation between VLT and energy savings, Pearson's correlation coefficient (r) was calculated [26]:

$$r = \frac{\sum \left(VLT_i - VLT\right)\left(Energy_{saved_i} - Energy_{saved}\right)}{\sqrt{\sum \left(VLT_i - VLT\right)^2 \cdot \sum \left(Energy_{saved_i} - Energy_{saved}\right)^2}} \tag{8}$$

A negative high correlation suggests that with increasing VLT, energy savings are reduced, emphasizing the compromise between daylighting and thermal performance.

3. Results and discussions

3.1. Annual energy and cost savings

The building's orientation plays a pivotal role in determining each of the façades' solar exposure, necessitating a specific film installation and shading strategy. As shown in Fig. 3, among all the alternatives evaluated, HD-IR05100 presents optimum performance and saves approximately

29,750 kWh/year. This is due to it possessing low VLT (5%) and high IRR (85%), strongly blocking SHG on sun-orientated façades such as the south orientation. HD-IR0590 and HD-IR20100 also make up for high performance with savings of almost 28,000 kWh/year, suggesting appropriateness for façades with moderate solar loads such as the west and east. HD-IR75100 gives the lowest energy savings, nearly 21,000 kWh/year. Though this film facilitates high daylight penetration in virtue of its high visible transmittance (75%), it is inefficient in reducing cooling loads and is thus more suitable than other films for north-facing facades where exposure to the sun is small. The overall trend supports a strong negative correlation between visible transmittance and energy savings, corroborating the trade-off between daylight availability and thermal performance. Such results emphasize the importance of façade-specific film use, where higher solar rejection films are applied to highly sun-exposed façades and daylighting-friendly films are applied where thermal loads are minimal. Such is in accordance with climate-responsive design, which provides for considerable energy savings through operational reductions without visual comfort compromise.

The bar chart shows the relative picture of the annual cost saving of the application of different nano-ceramic window films in a hot-arid climatic condition. The film type is shown on the x-axis (i.e., HD-IR0590, HD-IR20100), and the y-axis quantifies the amount of total cost saved per year in USD, calculated from the savings in cooling energy use.

As shown in Fig. 4, the highest C_{saved} are achieved by HD-IR05100 at approximately $3,570/year. This high performance is consistent with its very low VLT (5%) and high IRR (85%), which in combination significantly minimize SHG and thus cooling demand, effective for south- and west-oriented façades receiving much solar exposure throughout the year. Close seconds are HD-IR0590 ($3,400/year) and HD-IR20100 ($3,350/year), both also featuring high IR rejection (>80%) with relatively minor variation in transmittance. Conversely, HD-IR75100 ranks lowest in economic gain with a savings of about $2,550/year. This film has the highest VLT (75%) and prioritizes daylighting over solar control. While this kind of setup is perfect for north-facing façades where solar exposure is minimal, its use in high-gain façades translates to compromised thermal performance and therefore lower financial gain.

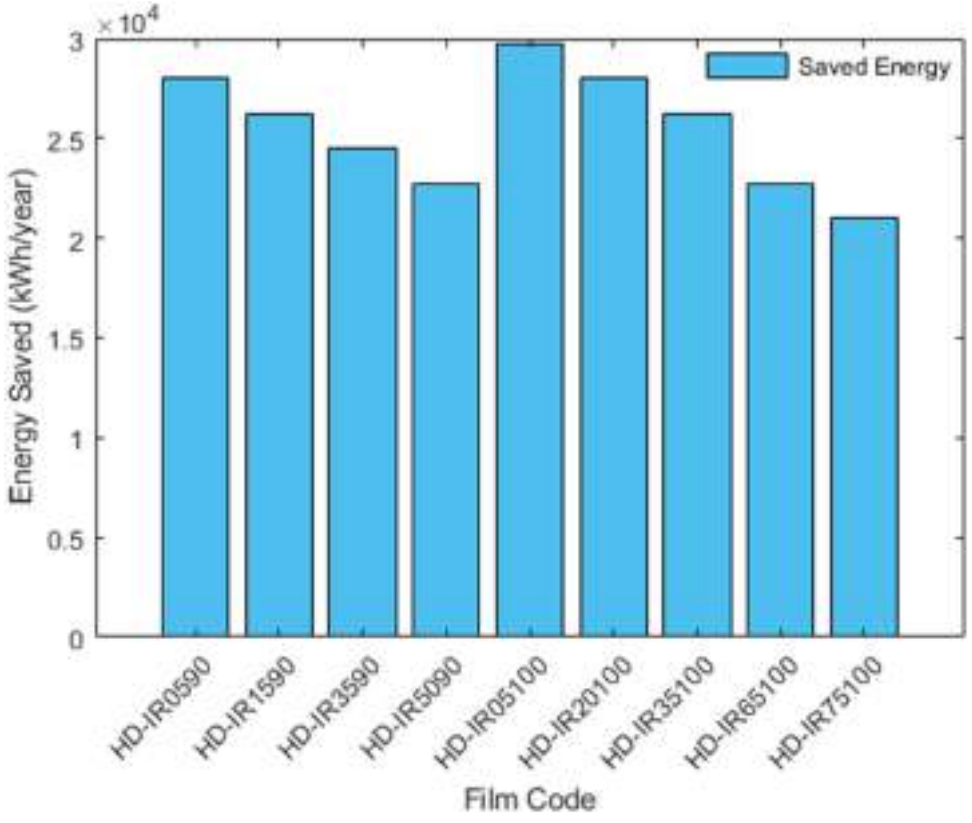

Fig. 3. Annual energy savings (kWh/year) resulting from the application of various nano-ceramic window films to a three-story commercial building in a hot-arid climate.

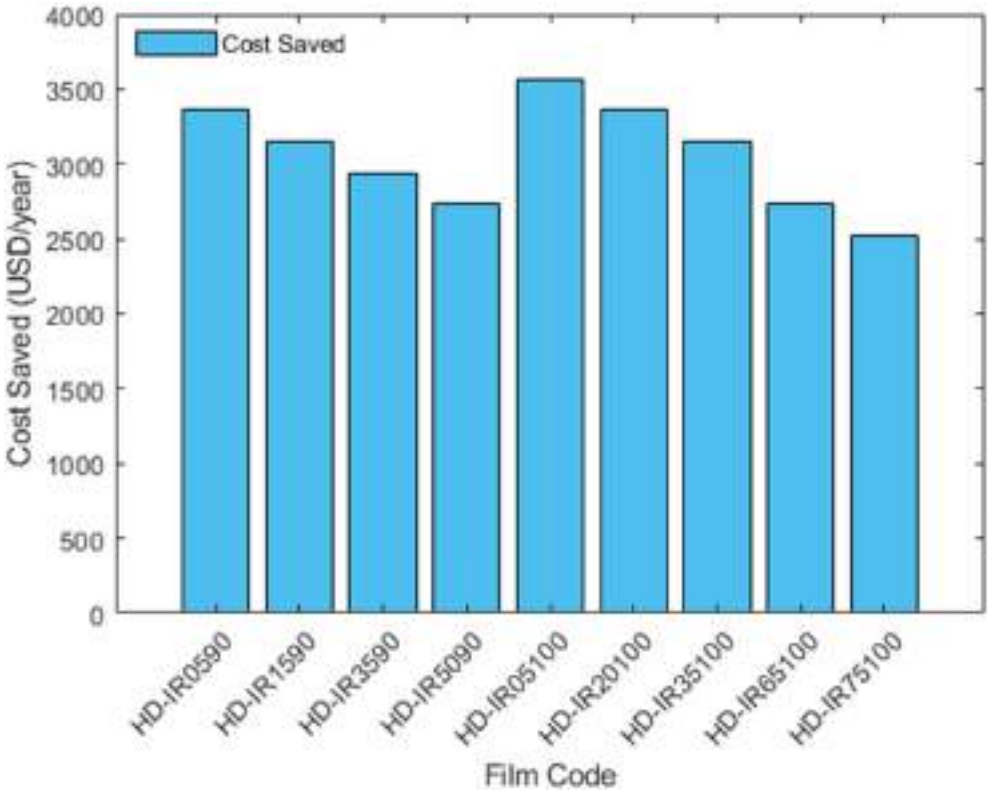

Fig. 4. Annual cost savings (USD/year) associated with various nano-ceramic window film types applied to a three-story commercial building in a hot-arid climate.

Mid-range products like HD-IR1590 ($3,200/year), HD-IR3590 ($2,950/year), and HD-IR5090 ($2,800/year) balance thermal protection and daylight transmittance and are therefore suitable for façades with moderate exposure such as the east and west orientations. Such films still yield significant operational savings and are therefore still viable choices in buildings where visual comfort or natural lighting is accorded high importance alongside energy performance.

A flat electricity rate of $0.12/kWh was used as a standardized reference value for estimating annual cost savings. This rate is not intended to represent Baghdad's subsidized or sector-specific tariffs, which may vary depending on building type and utility category. Under average commercial electricity, the savings illustrated here can translate to payback times of less than 2–3 years, especially for buildings with high cooling demand throughout the year. This renders nano-ceramic films an economically attractive retrofit or new-construction option for climate-adaptive architectural envelopes.

These economic results also guide façade-by-façade glazing approaches in early architectural design. High-return films like HD-IR05100 can be paired with shading devices for south and west façades, while HD-IR75100 and HD-IR65100 offer suitable daylight performance for north-facing zones like corridors, lobbies, or open-plan office areas. With the incorporation of economic and thermal performance data, architects and engineers can adopt an evidence-based approach to visual and thermal comfort optimization.

3.2. Integration with building aesthetics and functionality: Façade-specific SHG

The selection of the nano-ceramic films was not only with consideration to their thermal properties but also to their visual aspects to maintain the aesthetic integrity of the building relative to other materials [27]. The films are almost transparent, maintaining the exterior appearance of the building while providing enhanced interior comfort. Moreover, the ability of the film to block up to 99% of ultraviolet light protects interior furniture from fading, contributing to the building's interior design elements life expectancy.

Fig. 5 illustrates the average SHG (kWh/m^2/day) every month for the four predominant building façades. The South façade gets the highest solar gain from June to August, approximately 1.4 kWh/m^2/day, and therefore this is the optimal

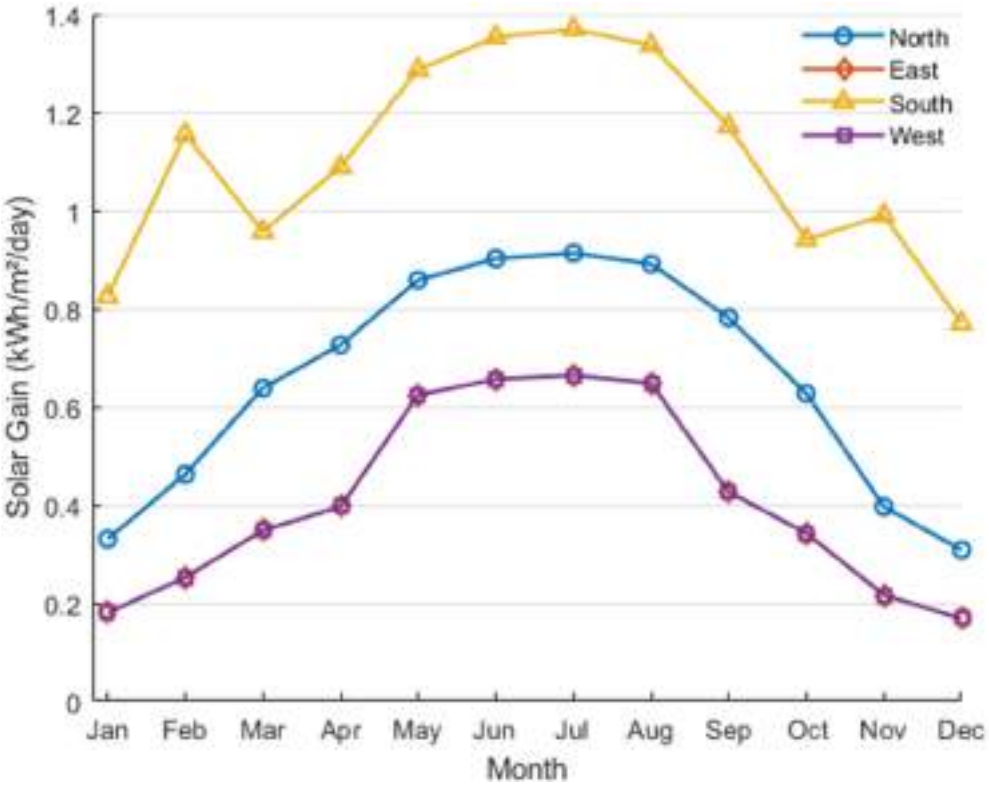

Fig. 5. Monthly average SHG (kWh/m^2/day) on each façade orientation of the simulated three-story building in Baghdad.

region to be targeted for thermal reduction. East and West fronts also show moderate gains from the sun, especially in morning and afternoon sun hours, reaching a peak in spring and autumn months due to low sun angles. Meanwhile, the North front is the least fluctuating and lowest exposed and rarely goes beyond 0.9 kWh/m^2/day. The monthly SHG analysis by various façades highlighted the south façade as solar-exposed to the maximum extent, and thus it was suitable for the use of low-transmittance film and horizontal shades [28]. East and west façades were augmented by vertical fins to fight low-angle sun, and the north façade, with low solar gain, was best suited for the use of high-VLT films to realize maximum daylighting. Such solar profiles have a direct application in architectural design decisions. High-performance solar control equipment, such as low-VLT, high-IRR films and exterior shading devices, are most justified on the South, East, and West façades. On the North façade, the comparatively low solar gain justifies the use of high-VLT films to maintain daylight penetration while inhibiting unnecessary thermal restriction.

All films demonstrated fine UVR (≥99%), providing protection against UV caused interior degradation as confirmed in Fig. 6. IRR, which is a key performance factor for heat, is above 90% for most films (e.g., HD-IR05100, HD-IR20100) and remains well within the expectations for thermal mitigation of high-gain façades. Interestingly, films such as HD-IR05100 and HD-IR0590 with IRR and NIR at 780–2500 nm of ~85–90% and ultra-low VLT of 5% are particularly appropriate for the South façade as they block the largest possible amount of solar heat while reducing glare, resulting in improved thermal comfort and energy savings. Conversely, high VLTs of 75% and 65% films HD-IR75100 and HD-IR65100 respectively are best suited to the North façade, where the maximum daylighting occurs, and thermal gain is minimum. The films also provide satisfactory IRR (~93%) and full UVR, while maintaining indoor comfort without any compromise on visual quality than in other studies [29].

While the optical performance values (e.g., UVR > 99%, IRR > 85%) are based on manufacturer- provided data, these represent optimal, as-manufactured conditions. Studies have shown that industrial products, including nano-ceramic coatings, can experience gradual degradation in optical properties over time due to UV exposure, thermal stress [30], and moisture [31]. For instance, long-term testing in hot-humid climates has shown IRR reduction of 5–10% over 5–7 years. Thus, the energy and daylighting performance reported here should be interpreted as representative of initial film performance, with possible variation under extended real-world aging.

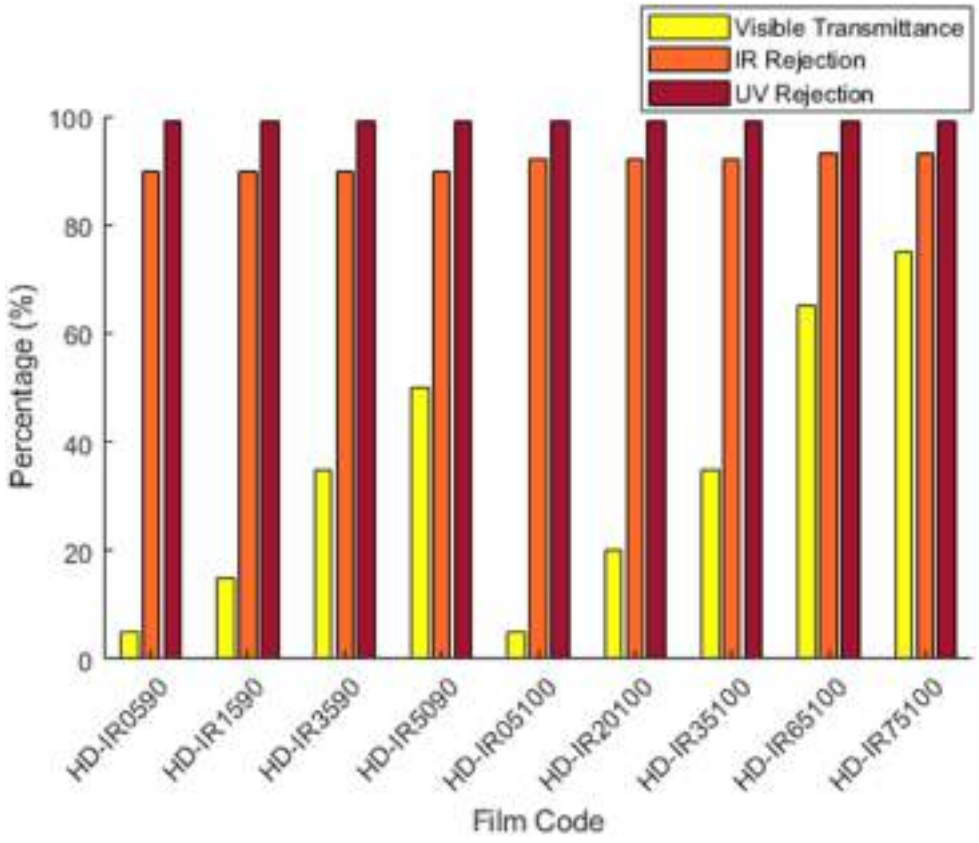

Fig. 6. Optical performance characteristics of nine nano-ceramic window films, showing percentages of VLT, IRR, and UVR. Note: Optical values are based on normal incidence; actual performance may vary with angle of solar radiation.

Table 2. Optical and thermal performance parameters of certain nano-ceramic window films, e.g., VLT, SR, and approximated annual energy savings.

Film Code	VLT (%)	SR (%)	Energy Saved (kWh/year)	Percent Savings (%)	kWh Saved per % VLT
HD-IR0590	5	80	28 000	80	5 600
HD-IR1590	15	75	26 250	75	1 750
HD-IR3590	35	70	24 500	70	700
HD-IR5090	50	65	22 750	65	455
HD-IR05100	5	85	29 750	85	5 950
HD-IR20100	20	80	28 000	80	1 400
HD-IR35100	35	75	26 250	75	750
HD-IR65100	65	65	22 750	65	350
HD-IR75100	75	60	21 000	60	280

3.3. Correlation between VLT and energy savings

An important inverse relationship ($r = -0.95$) is found between VLT and yearly energy savings. In Table 2, those films with smaller VLT percentages, like HD-IR05100 (5% VLT), show greater energy savings, amounting to 29,750 kWh/year. On the other hand, films such as HD-IR75100, with VLT 75%, produce smaller energy savings of 21,000 kWh/year. Such a trend highlights the balancing act between admitting natural light into a building and reducing SHG, which is important in cutting cooling loads. HD-IR05100 is the most efficient film. It saves 5,950 kWh of energy for every 1% of light it allows through. This means it provides a high level of energy savings even though it doesn't let in much light. On the other hand, HD-IR75100 saves only 280 kWh per 1% VLT. That means even though it lets in more light, it doesn't save as much energy per unit of light.

The energy savings observed are consistent with results from previous studies. For example, Huang published in 2024 a study where reflective films achieved up to 10.3% electricity-saving ratios varying with building orientation [32]. Similarly, research

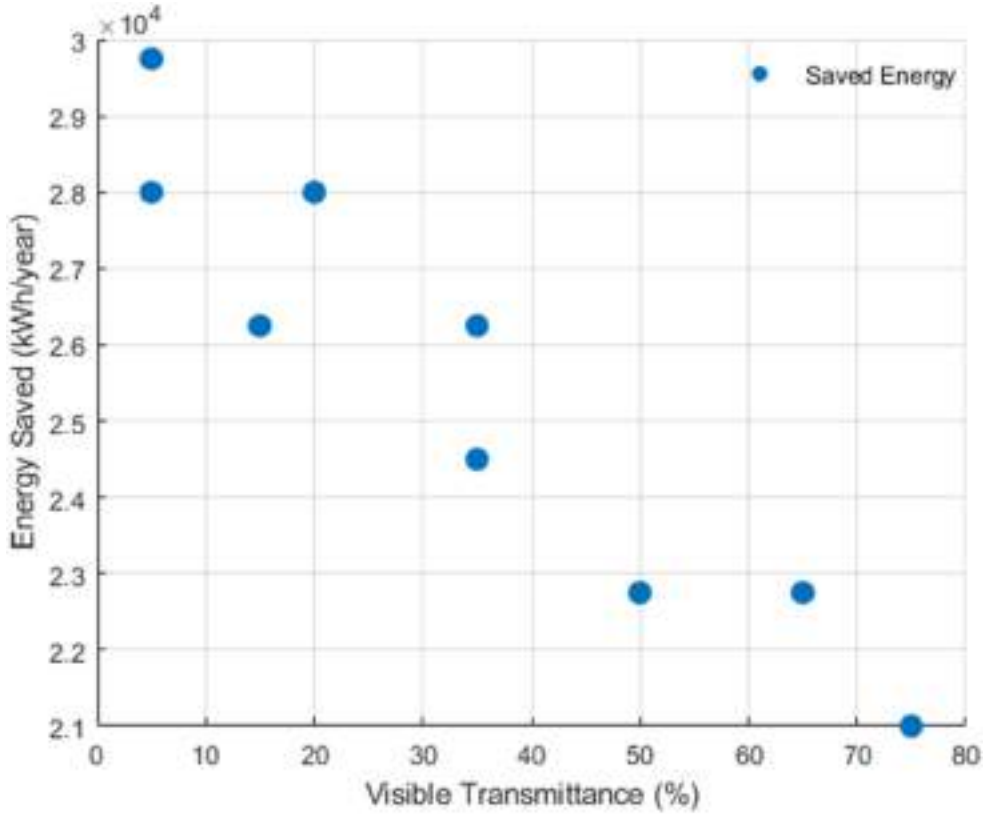

Fig. 7. The relationship between VLT (%) and annual E_{saved} (kWh/year) for different nano-ceramic window films.

work achieved by Bae et al. in 2024 introduced a directional radiative cooling glass that achieved over 1.5°C temperature reduction compared to regular glass, showcasing the potential of energy saving through enhanced window technology [33].

The architectural strategy was also extended to indoor space, where high VLT of certain films permitted penetration by daylight, reducing the requirement for artificial lighting. Not only does it cause energy saving but also contributes to the well-being of occupants by providing a perception of contact with the exterior environment [34]. The intelligent combination of film characteristics and shading devices maintains areas well-lit with no unpleasant glare, in line with sustainable building design best practice.

As shown in Fig. 7, high-VLT films like HD-IR75100 provided higher daylighting but resulted in lower $E_{savings}$ due to their limited IRR. Conversely, low-VLT films like HD-IR05100 achieved significantly greater energy savings, primarily because of their higher IRR values, which effectively reduced SHG and cooling loads, despite admitting less natural light. This compromise means sacrificing thermal performance against occupant comfort. While energy savings are better in low VLT films, they sacrifice indoor daylighting, which might affect occupant comfort in addition to requiring more artificial lighting. Therefore, selecting a window film is a trade-off between visual comfort and energy efficiency [35]. The mid-range VLT films such as HD-IR35100 (35% VLT) provide a compromise, which at high energy savings (26,250 kWh/year) will supply acceptable amounts of natural light [36].

4. Energy savings vs. CO_2 emissions

To quantify the environmental benefit of the energy savings achieved by the nano-ceramic films, the avoided CO_2 emissions were calculated by Eq. (5) using an emission factor of 0.65 kg CO_2/kWh, representative of Iraq's fossil fuel dominated grid. As shown in Table 3, the film HD-IR05100, with the lowest visible light transmittance (VLT = 5%), achieved the

Table 3. Annual energy savings and avoided CO_2 emissions per film type.

Film Type	VLT (%)	Energy Saved (kWh/year)	CO_2 Avoided (kg/year)
HD-IR05100	5	29,750	19,338
HD-IR35100	35	25,000	16,250
HD-IR75100	75	21,000	13,650

highest annual energy savings (29,750 kWh/year), corresponding to 19,338 kg CO_2 avoided per year. The HD-IR35100 and HD-IR75100 films resulted in 16,250 kg/year and 13,650 kg/year of CO_2 reduction, respectively. This analysis reveals a strong linear relationship between energy efficiency and environmental impact. Films with higher IR rejection (typically lower VLT) provide not only thermal and economic benefits but also meaningful reductions in greenhouse gas emissions, thus contributing to climate mitigation in hot-arid regions.

Although these films are lightweight and can be retrofitted onto existing glazing systems thus reducing material waste and embodied carbon compared to full window replacement their production may involve energy-intensive deposition techniques (e.g., sputtering), and their disposal poses recycling challenges due to mixed ceramic-polymer composition. Despite these limitations, the calculated avoided CO_2 emissions of up to 20.8 metric tons/year demonstrate a significant reduction in operational carbon footprint. This aligns with the goals of Sustainable Development Goal 7 (SDG 7) (Affordable and Clean Energy) and SDG 13 (Climate Action) by improving energy efficiency and reducing greenhouse gas emissions in buildings.

5. Limitations of the study

This case study is based on a single building type and climate zone (Baghdad, hot-arid), which may limit the generalizability of the results to other regions or building typologies. The optical properties used in simulations are based on manufacturer data under standard test conditions and do not account for long-term degradation or angle-dependent variation. Additionally, the analysis does not include embodied carbon or life cycle impacts of the films. Finally, HVAC operation and internal load assumptions were based on typical values due to limited access to site-specific energy data.

6. Conclusion

This study demonstrates that the application of nano-ceramic window films, when combined with climate-responsive architectural solutions, has the potential to significantly reduce building energy consumption without compromising daylight quality and occupant comfort. The research, carried out in a three-story commercial building model of 2,000 m^2 gross floor area and window-to-wall ratio of 40%, presents substantial annual energy savings ranging from 21,000 to 29,750 kWh/year, depending on the film. HD-IR05100 and HD-IR20100 films exhibited enhanced performance, rejecting up to 85% of solar radiation and providing maximum cost and energy savings for façades thermally exposed.

Architecturally, varied use of film per façade, high-transmittance on the north side, medium on east and west sides, and low-transmittance on the south side, was effective for optimizing energy performance without losing daylight availability. Shading devices like horizontal louvers and vertical fins further enhanced solar control, especially on east, west, and south orientations.

Correlation analysis revealed significant negative correlation ($r = –0.95$) between VLT measured and energy saved, supporting that higher VLT has the tendency to reduce thermal performance but increase daylight, highlighting the compromise inherent in glazing selection. Integration of an MCDA strategy allowed for appropriate selection on the basis of energy savings, daylight, cost, and durability.

Economically, the daily cost savings ranged from $1.50 to $2.80/day, which could amount to as much as over $1,000 savings in annual utility bills, making such movies cost-effective within a couple of years of construction. Environmentally, the cooling load savings indicates a substantial decrease in long-run marginal carbon emissions, which is supportive of green building certification and net-zero design efforts. Nano-ceramic films are not just reflective coatings but sophisticated building materials offering a high-performance, non-intrusive thermal control solution.

Future work should incorporate a formal Life Cycle Assessment (LCA) based on ISO 14040 standards to ensure that the environmental benefits of nano-ceramic films are sustained across all stages of their application.

Funding

Not Applicable.

Acknowledgment

The authors would like to express their sincere gratitude to Architect Zahraa Harith from the Renewable Energy and Environment Department – Research Office, Training and Research Office – Ministry of Electricity, Iraq, for her valuable technical input and support. The authors also acknowledge Al-Ayen Iraqi University (AUIQ) for its institutional support, which made this research possible.

Conflict of interest

The authors have no competing interests to declare that are relevant to the content of this article.

References

1. N. Barbieri and A. Palma, "Mapping energy-efficient technological advances in home appliances," *Energy Effic*, vol. 10, no. 3, pp. 693–716, Jun. 2017, doi: 10.1007/S12053-016-9470-7.
2. R. Khan, S. Ilyas, and Z. H. Doost, "Comparative assessment of land surface temperature in urbanized areas of the Saudi Arabia," *AUIQ Technical Engineering Science*, vol. 2, no. 1, Apr. 2025, doi: 10.70645/3078-3437.1027.
3. H. R. M. AL-agele, M. F. Z. Jaafar, and M. F. Shahidan, "Urban heat island effects and sustainable mitigation strategies in urban areas: Case study Jakarta City," *AUIQ Technical Engineering Science*, vol. 1, no. 1, Aug. 2024, doi: 10.70645/3078-3437.1006.
4. P. R. White, J. D. Rhodes, E. J. H. Wilson, and M. E. Webber, "Quantifying the impact of residential space heating electrification on the Texas electric grid," *Appl Energy*, vol. 298, Sep. 2021, doi: 10.1016/j.apenergy.2021.117113.
5. G. Mutezo and J. Mulopo, "A review of Africa's transition from fossil fuels to renewable energy using circular economy principles," Mar. 01, 2021, Elsevier Ltd. doi: 10.1016/j.rser.2020.110609.
6. A. Maté, J. Peral, A. Ferrández, D. Gil, and J. Trujillo, "A hybrid integrated architecture for energy consumption prediction," *Future Generation Computer Systems*, vol. 63, pp. 131–147, Oct. 2016, doi: 10.1016/j.future.2016.03.020.
7. R. N. Abed, M. Abdallh, A. Adnan Rashad, H. C. Al-Mohammedawi, and E. Yousif, "Spectrally selective coating of nanoparticles (Co3O4:Cr2O3) incorporated in carbon to captivate solar energy," *Heat Transfer*, vol. 49, no. 3, pp. 1386–1401, May 2020, doi: 10.1002/htj.21668.
8. N. Abundiz-Cisneros, R. Sanginés, R. Rodríguez-López, M. Peralta-Arriola, J. Cruz, and R. Machorro, "Novel Low-E filter for architectural glass pane," *Energy Build*, vol. 206, Jan. 2020, doi: 10.1016/j.enbuild.2019.109558.
9. I. Khan, "Importance of GHG emissions assessment in the electricity grid expansion towards a low-carbon future: A time-varying carbon intensity approach," *J Clean Prod*, vol. 196, pp. 1587–1599, Sep. 2018, doi: 10.1016/j.jclepro.2018.06.162.
10. L. Chen *et al.*, "The resilience paradox of rooftop PV: Building cooling penalties and heat risks," *Build Environ*, p. 113233, 2025.
11. Y. Lyu, J. Xiang, and H. Samuelson, "Carbon reductions through optimized solar heat gain glass properties considering future climate and grid emissions: case study of Chicago's residential buildings," *Energy Build*, vol. 327, p. 115080, Jan. 2025, doi: 10.1016/J.ENBUILD.2024.115080.
12. Zhang Hong, Gao Ping, Li Wentao, and Li Wenmei, "Method for preparing nano ceramic heat-insulating reflective coating," CN114702844A, 2022
13. Y. Cai *et al.*, "Utilization of translucent hydroxyapatite nanoceramics as a bio-window material," *Nano Advances*, pp. 45–49, Jun. 2016, doi: 10.22180/na169.
14. L. M. Shaker, "Evaluating UV-protective low-emissivity window films: implications for thermal and visual comfort in luminous office buildings," *AUIQ Complementary Biological System*, vol. 1, no. 2, pp. 46–60, Oct. 2024, doi: 10.70176/3007-973X.1014.
15. S. K. A., D. R. Darul, M. K. Mohamed, and K. D. Arunachalam, "Industrial applications of nanoceramics: from lab to real-time utilization—The environmental, legal, health, and safety issues of nanoceramics," *Industrial Applications of Nanoceramics*, pp. 411–423, Jan. 2024, doi: 10.1016/B978-0-323-88654-3.00027-5.
16. A. Sedaghat *et al.*, "Effects of window films in thermo-solar properties of office buildings in hot-arid climates," *Front Energy Res*, vol. 9, May 2021, doi: 10.3389/fenrg.2021.665978.
17. A. P. Čuden and R. Urbas, "Advances in ultraviolet (UV) ray blocking textiles," in *Functional and Technical Textiles*, Elsevier, 2023, pp. 213–273. doi: 10.1016/B978-0-323-91593-9.00013-4.
18. E. Shen, J. Hu, and M. Patel, "Energy and visual comfort analysis of lighting and daylight control strategies," *Build Environ*, vol. 78, pp. 155–170, Aug. 2014, doi: 10.1016/J.BUILDENV.2014.04.028.
19. M. Al-Riahi, N. Al-Hamdani, and H. Al-Saffar, "Some aspects of solar radiation climatology of Iraq," *Renew Energy*, vol. 2, no. 2, pp. 167–173, Apr. 1992, doi: 10.1016/0960-1481(92)90102-9.
20. F. M. Abed, Y. Al-Douri, and G. M. Y. Al-Shahery, "Review on the energy and renewable energy status in Iraq: The outlooks," *Renewable and Sustainable Energy Reviews*, vol. 39, pp. 816–827, 2014, doi: 10.1016/j.rser.2014.07.026.
21. M. G. Hutchins, "Spectrally selective materials for efficient visible, solar and thermal radiation control," in *Solar Thermal Technologies for Buildings: The State of the Art*, CRC Press, 2014, pp. 37–64. doi: 10.4324/9781315074467.
22. International Organization for Standardization, *ISO 9050: Glass in building — Determination of light transmittance, solar direct transmittance, total solar energy transmittance, ultraviolet transmittance and related glazing factors*. 2003.
23. C. A. Gueymard, D. Myers, and K. Emery, "Proposed reference irradiance spectra for solar energy systems testing," *Solar Energy*, vol. 73, no. 6, pp. 443–467, 2002, doi: 10.1016/S0038-092X(03)00005-7.
24. J. E. Braun and J. C. Mitchell, "Solar geometry for fixed and tracking surfaces," *Solar Energy*, vol. 31, no. 5, pp. 439–444, 1983, doi: 10.1016/0038-092X(83)90046-4.
25. H. Samuelson, C. Srivastava, and A. Baniassadi, "Optimizing window solar heat gain coefficient for energy and carbon performance in a changing context of electrification and decarbonization," *Energy Reports*, vol. 13, pp. 1450–1466, Jun. 2025, doi: 10.1016/J.EGYR.2025.01.013.
26. A. G. Dufera, T. Liu, and J. Xu, "Regression models of pearson correlation coefficient," *Stat Theory Relat Fields*, vol. 7, no. 2, pp. 97–106, 2023, doi: 10.1080/24754269.2023.2164970.
27. D. G. Kim, B. Jung, K. H. Kim, K. Y. Cho, and Y. C. Jeong, "Highly robust and transparent flexible cover window films based on UV-curable polysilsesquioxane nano sol," *J Appl Polym Sci*, vol. 137, no. 35, p. 49012, Sep. 2020, doi: 10.1002/app.49012.
28. S. Kim, M. Bayatvarkeshi, A. M. Ali, and K. Ahmed, "Decadal climate and landform variables analysis in iraq using remote sensing datasets," *AUIQ Technical Engineering Science*, vol. 1, no. 2, Dec. 2024, doi: 10.70645/3078-3437.1013.
29. A. Sedaghat *et al.*, "Experimental study on the performance of solar window films in office buildings in Kuwait," *Journal of Nanoparticle Research*, vol. 22, no. 4, pp. 1–17, Apr. 2020, doi: 10.1007/s11051-020-04789-8.

30. Y. Gu, K. Xia, D. Wu, J. Mou, and S. Zheng, “Technical characteristics and wear-resistant mechanism of nano coatings: A review,” *Coatings*, vol. 10, no. 3, Mar. 2020, doi: 10.3390/coatings10030233.
31. R. Roshan, S. K. Patel, and A. Behera, “Future perspective of ceramic coating,” *Advanced Ceramic Coatings for Energy Applications*, pp. 325–341, Jan. 2024, doi: 10.1016/B978-0-323-99620-4.00014-2.
32. H. Y. Huang *et al.*, “Evaluation of the effects of window films on the indoor environment and air-conditioning electricity consumption of buildings,” *Energies (Basel)*, vol. 17, no. 6, Mar. 2024, doi: 10.3390/en17061388.
33. M. Bae, D. H. Kim, S. K. Kim, and Y. Min Song, “Transparent energy-saving windows based on broadband directional thermal emission,” *Nanophotonics*, vol. 13, no. 5, pp. 749–761, Mar. 2024, doi: 10.1515/nanoph-2023-0580.
34. J. Wang and D. Shi, “Spectral selective and photothermal nano structured thin films for energy efficient windows,” Dec. 15, 2017, Elsevier Ltd. doi: 10.1016/j.apenergy.2017.10.066.
35. J. Pereira, M. Glória Gomes, A. Moret Rodrigues, H. Teixeira, and M. Almeida, “Small-scale field study of window films’ impact on daylight availability under clear sky conditions,” *Journal of Facade Design and Engineering*, vol. 8, no. 1, pp. 65–84, 2020, doi: 10.7480/jfde.2020.1.4785.
36. K. Park, S. Jin, and G. Kim, “Transparent window film with embedded nano-shades for thermoregulation,” *Constr Build Mater*, vol. 269, Feb. 2021, doi: 10.1016/j.conbuildmat.2020.121280.